NASA Technical Paper 3307

1992

Structurally Adaptive Space Crane Concept for Assembling Space Systems on Orbit

John T. Dorsey,
Thomas R. Sutter,
and K. Chauncey Wu
Langley Research Center
Hampton, Virginia

National Aeronautics and Space Administration
Office of Management
Scientific and Technical Information Program

Nomenclature

ACCESS	Assembly Concept for Construction of Erectable Space Structures
DOF	degree of freedom
FTS	Flight Telerobotic Servicer
ISCF	in-space construction facility
LEO	low Earth orbit
LTV	lunar transfer vehicle
MTV	Mars transfer vehicle
PSCI	preshaped command input
RMS	remote manipulator system
SEI	Space Exploration Initiative
SPDM	Special Purpose Dexterous Manipulator
SSRMS	Space Station *Freedom* remote manipulator system
TMS	tip manipulator system
VGT	variable-geometry truss

Abstract

Many future human space exploration missions will probably require large vehicles that must be assembled on orbit. Thus, a device that can move, position, and assemble large and massive spacecraft components on orbit becomes essential for these missions. This paper describes a concept for such a device—a space crane concept that uses erectable truss hardware to achieve high-stiffness and low-mass booms and uses articulating-truss joints that can be assembled on orbit. The hardware has been tested and shown to have linear load-deflection response and to be structurally predictable. The hardware also permits the crane to be reconfigured into different geometries to satisfy future assembly requirements. A number of articulating and rotary joint concepts have been sized and analyzed, and the results are discussed in this paper. Two strategies have been proposed to suppress motion-induced vibration: placing viscous dampers in selected truss struts and preshaping motion commands. Preliminary analyses indicate that these techniques have the potential to greatly enhance structural damping.

Introduction

Future human missions proposed for the Space Exploration Initiative (SEI) include establishing a lunar base and exploring Mars (ref. 1). Because these missions will not occur for many years, the missions, together with the spacecraft necessary to accomplish them, are not well-defined. Currently, many different configurations are being investigated for the lunar and the Mars transfer vehicle (LTV and MTV). Table 1 lists the total mass and reference dimensions for representative configurations. (See refs. 2 and 3.) One feature typical of these proposed spacecraft is that they are too large and massive to be placed into low Earth orbit (LEO) as a complete unit by a single launch of any current U.S. launch vehicle or even by a single launch of any proposed heavy-lift launch vehicle. (See table 1.) Consequently, these spacecraft must be assembled in LEO with a device such as a space crane (ref. 4). Assembly could take place at a space station or at a separate in-space construction facility (ISCF), as illustrated in figure 1(a), or the transfer vehicle itself could serve as the assembly platform, as illustrated in figure 1(b). Major uses of the space crane include moving large vehicle components together for assembly (or apart for disassembly), moving components from the delivery vehicle to a construction site, moving the entire vehicle, or helping service and process reusable LTV's and MTV's. Because on-orbit assembly operations and facilities that require a crane are not well-defined, the space crane concept should provide a generic assembly capability that can be developed independently of any one spacecraft concept, construction scenario, or available on-orbit assembly infrastructure.

Table 1. Parameters for Proposed SEI Spacecraft and U.S. Launch Vehicles

(a) SEI spacecraft parameters

Spacecraft	Total mass, lbm	Reference dimensions	
		Diameter, ft	Length, ft
Lunar transfer vehicle (with aerobrake)	420 000–490 000	50	75
Mars transfer vehicle (with aerobrake)	1 900 000	110	170
Nuclear Mars vehicle	1 900 000	98	360

(b) U.S. Launch vehicle parameters

Launch vehicle	Mass to low Earth orbit, lbm	Payload shroud size	
		Diameter, ft	Length, ft
Space Shuttle[a]	43 000	15	60
Titan 4[a]	39 000	16.7	65
Shuttle C[b]	150 000	15	82
National launch system[b]	300 000	41	98
Heavy-lift launch vehicle[b]	300 000	41	98

[a]Operational.

[b]Proposed.

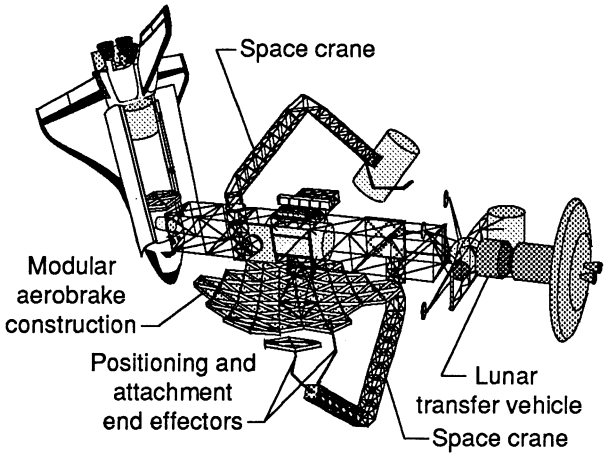

(a) In-space construction facility with cranes.

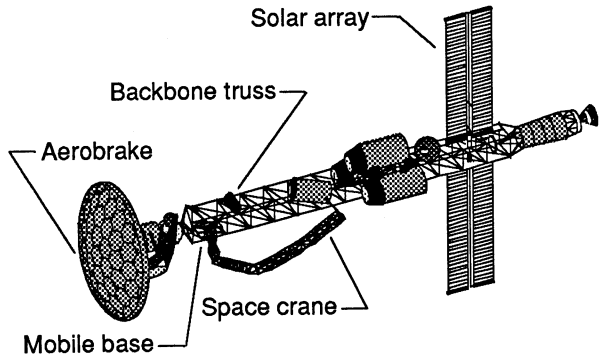

(b) Self-assembled Mars transfer vehicle.

Figure 1. On-orbit assembly of large spacecraft.

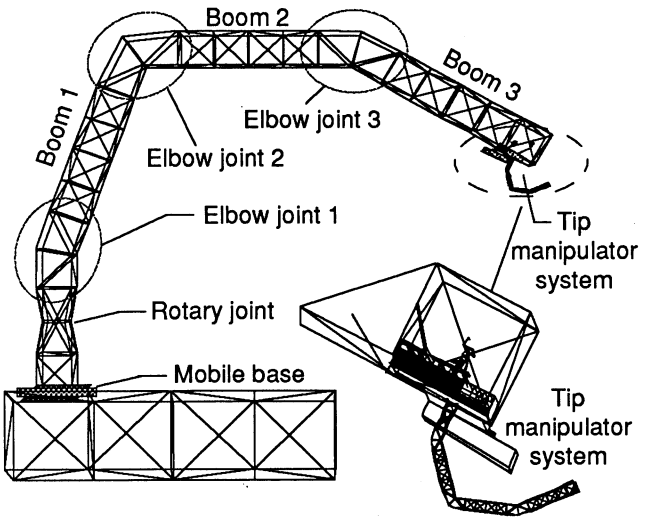

Figure 2. Space crane concept.

In general, a space crane system, such as the one shown in figure 2, is anticipated to have three major elements: (1) a mobile base that can move around the work site (ref. 5), (2) a crane body that consists of booms and articulating-truss joints to provide coarse tip positioning over large distances, and (3) a tip manipulator system (TMS) that provides additional dexterity and precisely positions payloads. Initially, the TMS can be used to help assemble the components of the crane body. The TMS can also be mounted to a mobile base so that it can translate along the crane body. The representative space crane body shown in figure 2 has three truss booms and a total of four articulating joints: three single-degree-of-freedom (DOF) elbow joints connecting the booms and a single-DOF rotary joint connecting the base of the crane body to the mobile base.

For a space crane to be viable for large-scale on-orbit assembly operations, it must possess several key features. The most important feature is that it be structurally adaptable, which is defined here as the ability of the structure to be reconfigured to adapt to changing operational requirements. A second feature is that it be structurally predictable. This feature is important because it is difficult and costly to perform ground-based tests on a complete full-scale system that has been designed to operate in zero-gravity (ref. 4). Structural predictability is also important because it can simplify the design of the control system. Other features the space crane should exhibit are the ability to move large masses within a required acceleration envelope, long reach, and easily implemented passive damping for vibration suppression. Because current manipulators for space applications exhibit none of these features, their applicability for on-orbit assembly of MTV and LTV spacecraft is limited. This paper describes a space crane concept that exhibits all these features. This paper also summarizes the current structural hardware applicable to the space crane body and the results of experimental and analytical studies to characterize structural behavior of the body components. The mobile base and tip manipulator system elements of the space crane are not discussed in this paper.

Operational and Proposed Space Manipulators

Figure 3 shows one operational and four proposed in-space manipulator systems having the broad range of performance characteristics listed in table 2. These manipulator systems include the Space Shuttle remote manipulator system (RMS, refs. 6–8) the Space Station *Freedom* RMS (SSRMS, ref. 9), the Special Purpose Dexterous Manipulator (SPDM, ref. 9), the

Flight Telerobotic Servicer (FTS, refs. 10 and 11), and a variable-geometry truss manipulator called the TRUSSARM (ref. 12). The Space Shuttle RMS (see fig. 3(a)) is the only manipulator system currently operational, and it has been used during many Shuttle missions over the last decade. The RMS, SSRMS (fig. 3(b)), FTS (fig. 3(c)), and SPDM (fig. 3(d)) are all derived from the same basic concept; that is, high-stiffness tubular booms are connected together by rotary joints driven by motors with mechanical gearboxes. As a structural component, these rotary joints are relatively flexible and exhibit nonlinear structural behavior because the load path through the joints is typically complex and involves many mechanisms. (See, for example, the RMS elbow joint shown in fig. 4(a).)

Another feature of these rotary joints is that the drive and pivot are generally close together; therefore, the overall stiffness of the manipulators is reduced because the equivalent area moment of inertia is small. These joints are usually not lightweight, and the total joint mass can be a large percentage of the manipulator mass. In the RMS, for example, the rotary joints comprise about 60 percent of the total mass (ref. 8). Scaling the size of these rotary joints to achieve higher stiffness would probably result in a significant increase in joint mass. A common deficiency among the manipulators listed in table 2 is that a given configuration is not easily modified to adapt to changing requirements because the number of degrees of freedom, booms, and joints is fixed (although reconfiguration was considered in the design of the FTS). Also, the positioning devices generally lack either the capability to handle massive spacecraft components or the reach required to assemble the proposed spacecraft listed in table 1.

The TRUSSARM (ref. 12), shown in figure 3(e), represents a class of adaptive structures, known as variable-geometry truss (VGT) structures, with a large number of degrees of freedom. (See ref. 13.) The TRUSSARM differs significantly from the previous manipulator systems in that the concept incorporates high-stiffness, high-strength, and low-mass truss structures. Linear actuators, located in the batten frame members, are extended to provide the necessary positioning capability. (Linear actuators are defined as actuators that provide extension in one DOF along the axis of the actuator.)

Conceptually, the TRUSSARM contains three actuators in each batten frame, and selected batten members can be extended or retracted to provide articulation about two axes and linear extension along the truss centerline of each batten frame. Truss members must have hinges (with one or more DOF) near or at the nodes to accommodate the required degrees of freedom of the truss. A typical TRUSSARM configuration uses a total of 99 actuators. (See ref. 13.) This large number of degrees of freedom may be unnecessary for most on-orbit assembly tasks. Furthermore, the large number of hinges and actuators in a TRUSSARM may lead to poor structural predictability and significant nonlinearity for this manipulator.

Table 2. Characteristics of Operational and Proposed Space Manipulators

Space manipulators	Payload, lbm	Tip force, lbf	Tip velocity, in/sec	Positioning accuracy		DOF	Reach, in.	Weight, lbm
				± in.	± deg			
RMS (operational)	65 000	12	2.40–24.00	2.00	1.0	6	603.0	966
SSRMS (proposed)	255 200	[a]10	[a].47–14.60	1.80	.7	7	694.0	[b]3834
SPDM (proposed)	1 200	25	[a].60–1.20	.05	[c].5	[d]19	[e]78.4	1800
FTS (cancelled)	1 200	20	24.00	1.00	3.0	[d]14	[e]60.0	[f]1500

[a]Not finalized.
[b]Includes flight-support equipment.
[c]With artificial vision.
[d]Total for both arms.
[e]For each arm.
[f]Not to exceed for all flight elements.

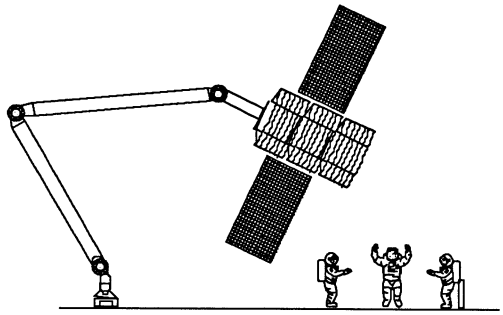

(a) Space Shuttle RMS.

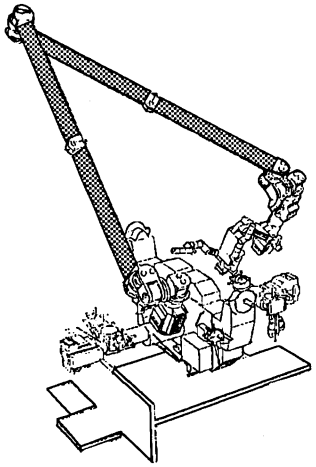

(b) Space Station *Freedom* RMS.

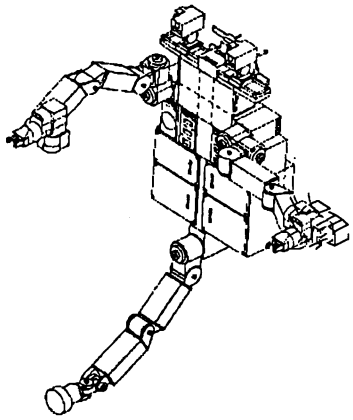

(c) FTS.

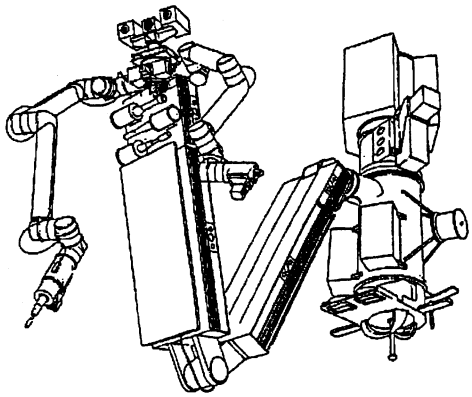

(d) SPDM.

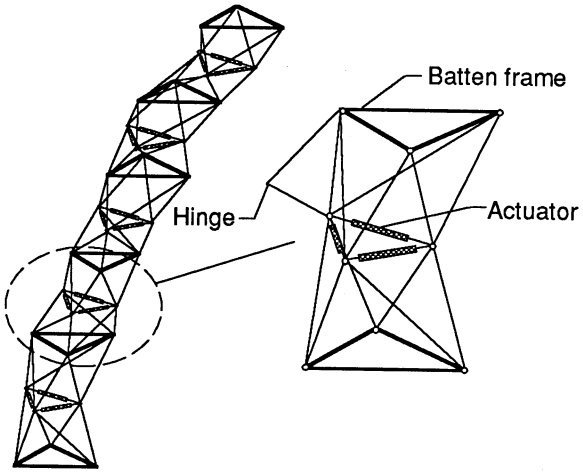

(e) TRUSSARM.

Figure 3. Operational and proposed space manipulators.

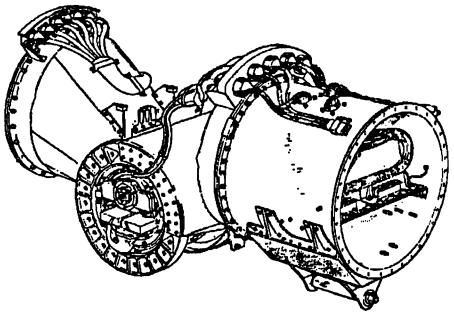

(a) Space Shuttle RMS elbow joint.

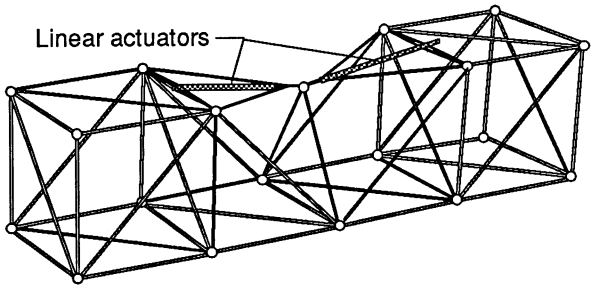

(b) Space crane elbow joint.

Figure 4. Elbow joint concepts.

Structural Concept

The space crane presented in this paper uses a structural concept different from that of the RMS, SSRMS, FTS, and SPDM. The space crane booms are trusses, which generally possess significantly higher flexural and torsional stiffnesses than do solid or tubular beams of the same length and mass. Using truss booms allows lightweight space cranes to be constructed with large reach envelopes. The space crane articulating-truss joints are designed to permit boom rotation without a significant reduction in stiffness (ref. 14). The space crane elbow joint, shown in figure 4(b), incorporates linear actuators as variable-length truss elements. The joint achieves articulation through actuator length change accompanied by rotation of simple pin connections between adjacent truss members. The space crane rotary joint (fig. 5(a)) incorporates an annular bearing race and discrete-bearing assemblies, which connect to the booms through transition truss sections. Because the elements are primarily loaded in tension and compression, these articulating-truss joint concepts exhibit inherently simpler load paths than do the complex joint mechanisms used in the RMS and similar systems. Hence, joint stiffnesses and strengths can be accurately predicted from tension-compression tests of each element.

Many different configurations exist for both the space crane booms and the articulating-truss joints, and different combinations of joints and booms can be assembled to produce a variety of capabilities. The truss booms, for example, can be constructed with either the four-longeron or the three-longeron concepts shown in figure 5(b). An advantage of the four-longeron boom is the structural redundancy provided by the fourth longeron. However, the three-longeron truss boom provides a lower part count and a more natural transition to certain articulating joint concepts. In addition to the articulating-truss elbow and rotary joints described previously, variable-geometry truss joints (fig. 5(a)) can be used if more than one DOF is needed at a particular joint location. Also, a two-DOF articulating-truss joint can be constructed by connecting a rotary and an elbow joint together.

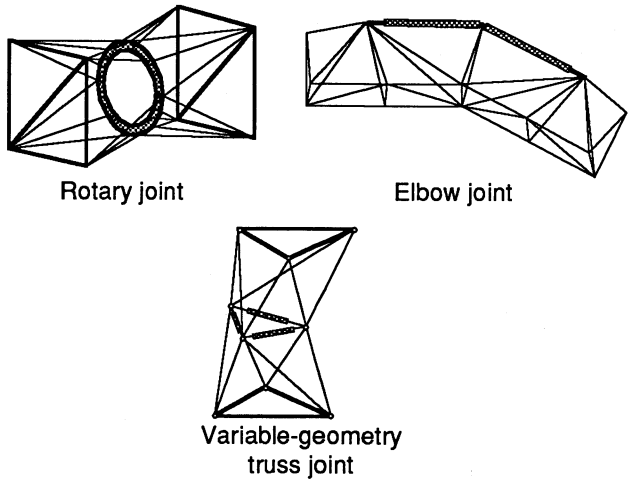

(a) Articulating-truss joint concepts.

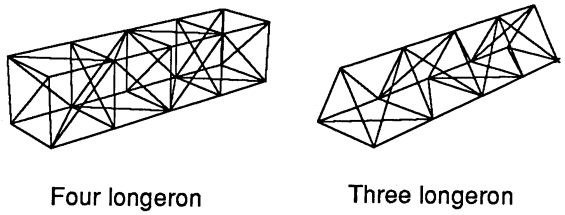

(b) Truss boom concepts.

Figure 5. Space crane components.

The costs for space missions may be significantly reduced if the structural concepts use or adapt previously developed space-qualified hardware, use modular components, and are adaptable. The current space crane concept is developed around proven erectable truss hardware, which is described in reference 15. This hardware can be easily and quickly

assembled, disassembled, and reconfigured into different geometries. Therefore, the space crane has the adaptability to meet a variety of assembly situations. For example, truss booms and articulating joints can be added or removed, or existing truss booms can be lengthened or shortened. Also, additional joints (and their associated DOF's) can be used to add dexterity or redundancy for rigid-body positioning.

The erectable truss joint is an example of a generic structural concept because the hardware is easily scaled for different applications. Currently, three sizes of erectable truss joints (1-, 2-, and 4-in-diameter joints have been designed and fabricated from 7075-T6 aluminum. (See fig. 6.) The 1- and 2-in-diameter joints are considered state of the art because they have been used for several ground-based assembly and structural tests (refs. 15–17). The 4-in-diameter joint is in the prototype stage of development, and it is being designed for applications that require heavily loaded members. The joints shown in figure 6 have been characterized in load-deflection tests, and the stiffness (EA) and ultimate load (F_{ult}) for each joint are noted in the figure. Using erectable truss hardware allows the truss bay depth (and associated bending stiffness) to be scaled where required. Also, the truss beam can be locally stiffened simply by replacing selected struts. Similarly, truss members with higher buckling strength can be substituted for the standard components in highly loaded areas of the space crane. Advance development work is underway at the Langley Research Center to develop truss joints with a low coefficient of thermal expansion. This effort is directed at fabricating the primary load-bearing components in these erectable truss joints from braided graphite preforms impregnated with a suitable matrix.

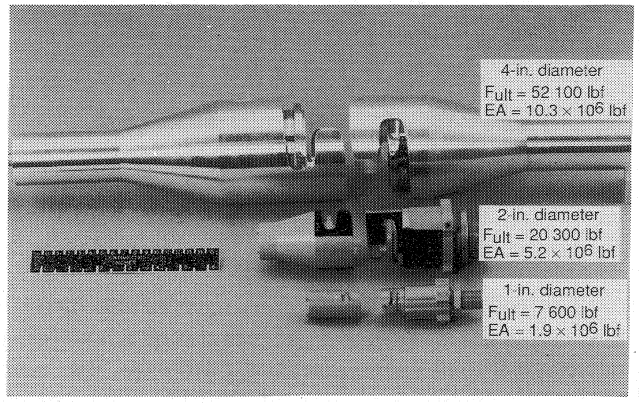

L-90-11950

Figure 6. Erectable truss joint hardware. F_{ult} indicates ultimate load and EA indicates stiffness.

Structural Component Analysis and Testing

This section presents a summary of analytical and experimental results from development studies of the space crane body and its components.

Truss Booms

Figure 7 shows a truss boom test article assembled from eight cubic-truss bays, each 39.4 in. long, and cantilevered from a structural backstop. This eight-bay test unit was chosen to establish a performance baseline for comparing static and dynamic test results on the articulating-truss joint (ref. 16). The truss boom was constructed with erectable truss hardware, which consists of struts, erectable joint hardware, and truss nodes. The 1-in. erectable joint hardware shown in figure 6 was used to make the structural connection between the struts and the truss nodes, and the struts were made of 1-in-diameter aluminum tubes with wall thicknesses of 0.058-in. For space applications, the struts will probably be constructed of high-stiffness graphite/epoxy tubes, which are similar to those described in references 18 and 19.

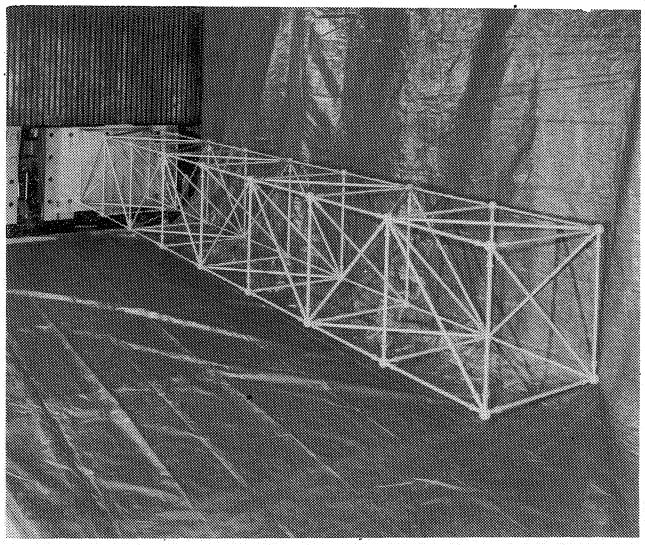

L-92-08955

Figure 7. Truss boom test hardware.

The static load-deflection behavior and the modal characteristics were experimentally determined for the truss boom and are compared with linear finite-element analysis results in figures 8(a) and 8(b), respectively. For the static test, the truss boom was loaded three bays inboard from the tip, and the corresponding deflections were measured one bay inboard from the tip. The truss boom was loaded to ±270 lbf

for three cycles to obtain the load-deflection curve shown in figure 8(a). The load-deflection response is linear with very little hysteresis over the entire load range. The slope of the load-deflection response is about 445 lbf/in., which is within 1 percent of the analytical predicted slope of 446 lbf/in. obtained from linear finite-element analysis. This close agreement between the experimental and analytical stiffnesses suggests excellent static predictability and linearity for the erectable truss hardware.

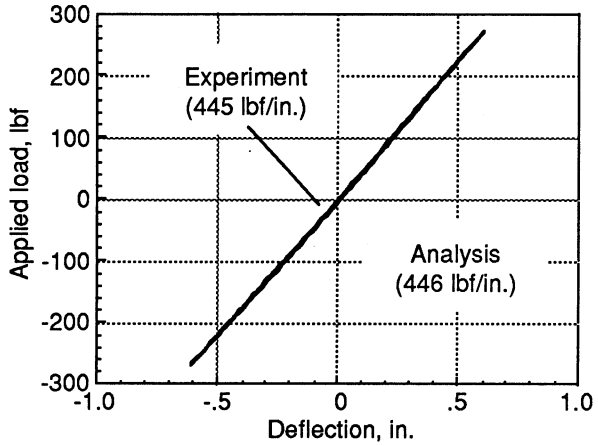

(a) Load-deflection response.

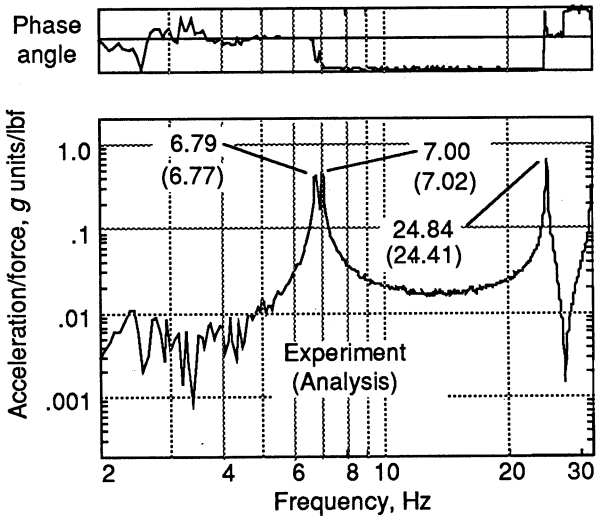

(b) Measured frequency response.

Figure 8. Truss boom response to static and dynamic loading.

The modal characteristics were obtained by applying random forces (from vibration exciters) at the truss nodes and by measuring the resulting acceleration time response. Experimental frequencies were obtained with the frequency response functions, and the experimental mode shapes were obtained with commercial modal analysis software. Figure 8(b) shows a typical experimental frequency response function for the truss boom. The three distinct frequency peaks at 6.79, 7.00, and 24.84 Hz correspond to the two first bending modes and the first torsion mode. The erectable truss hardware had very low structural damping, with each of the experimental modes having a modal damping value of less than 0.60 percent. The analytically predicted frequencies for the lowest three modes were 6.77, 7.02, and 24.41 Hz. The good correlation between the experimental and analytical results confirms that the structural performance of the erectable truss hardware is repeatable, because the static and dynamic performance was accurately predicted with experimental stiffness data reported previously in reference 15. The correlation also indicates that linear analysis can accurately predict the dynamic performance of longer beams or beams of different configurations fabricated with the erectable truss hardware.

Articulating-Truss Joints

Elbow joints. The articulating-truss joint test hardware shown in figure 9 consists of a first-generation elbow joint located between two truss booms. The first truss boom, which is connected at one end to a structural backstop, consists of two cubic-truss bays, each 39.4 in. long, and the second truss boom consists of four cubic-truss bays. The same 1-in-diameter erectable hardware described in the previous section is also used in this test model. A transition truss structure is required to connect the four-longeron truss booms to the three-longeron articulating-truss joint. The articulating-truss joint has only three longerons to avoid having to synchronize two parallel actuators during joint articulation. The two linear actuators in the articulating-truss joint have been extended to produce a 90° angle in the test model, as shown in the inset of figure 9. The joint is equivalent in length to two truss bays, and it has seven hinges, two actuator support beams (labeled beam in fig. 9), two linear actuators, and erectable truss hardware. The hinges allow the joint to rotate as the linear actuators are extended. Three hinges are located at each vertex of the joint A-frame, and the other four hinges are located near each end of the support beams. The A-frame maintains the truss cross-sectional depth as the joint rotates and stabilizes the three hinges located at each apex. The A-frame is connected to the two linear actuators by a hinge. The two actuator support beams are attached to the end of each linear actuator. The two linear actuators provide the extension needed to rotate the joint, and each has a mass of about 26.0 lbm. These actuators are inexpensive devices chosen to evaluate

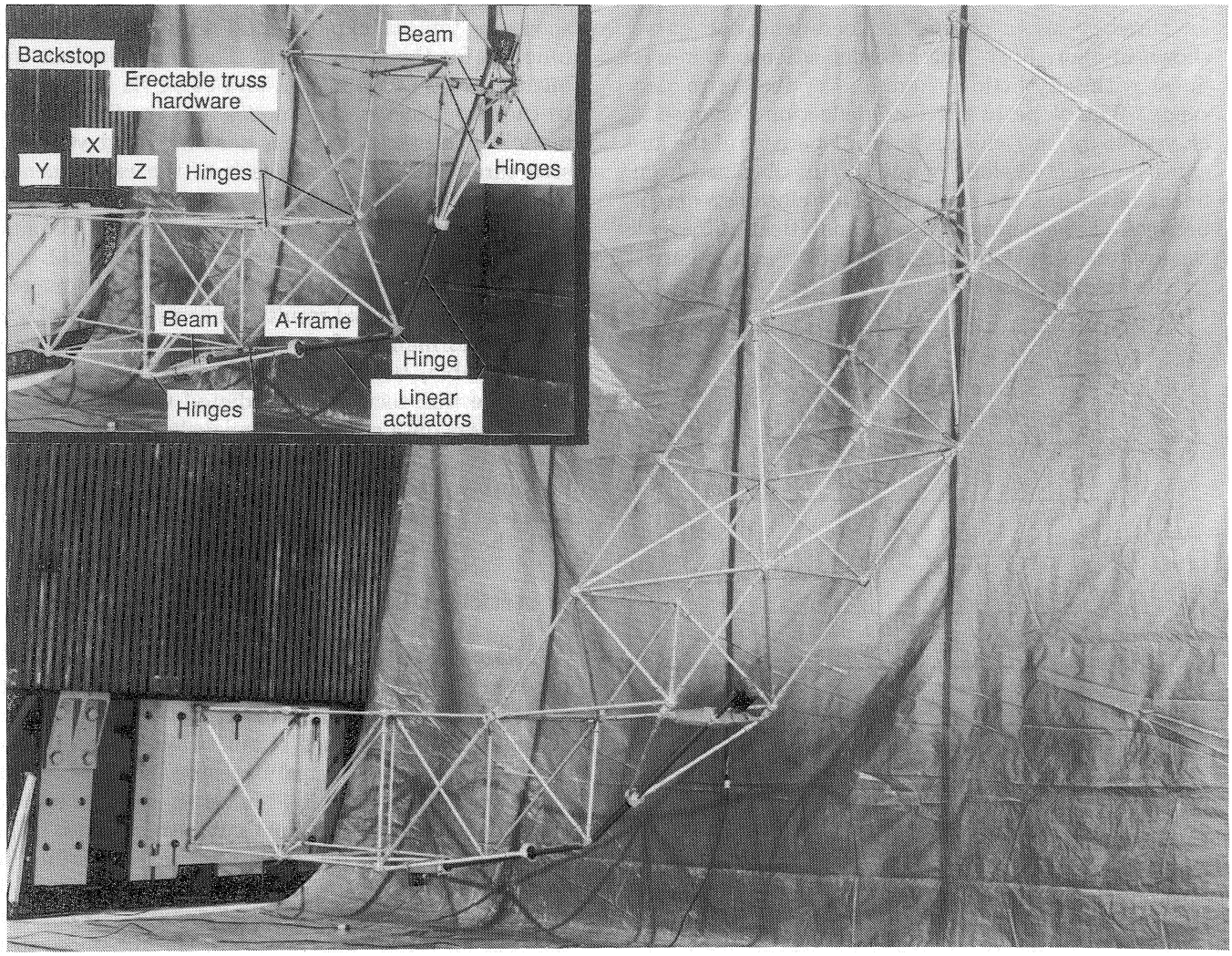

Figure 9. First-generation elbow truss joint test hardware.

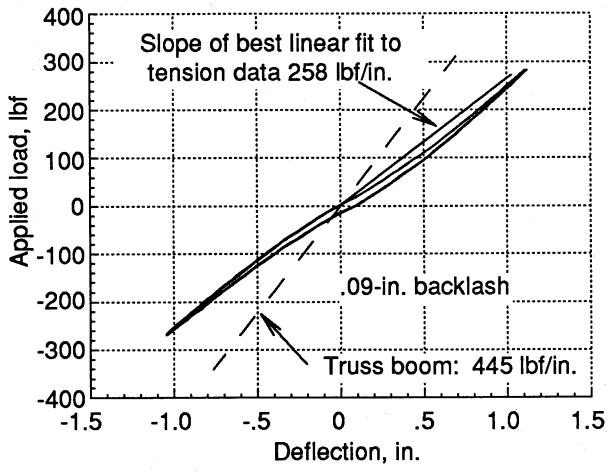

(a) Elbow joint with actuators.

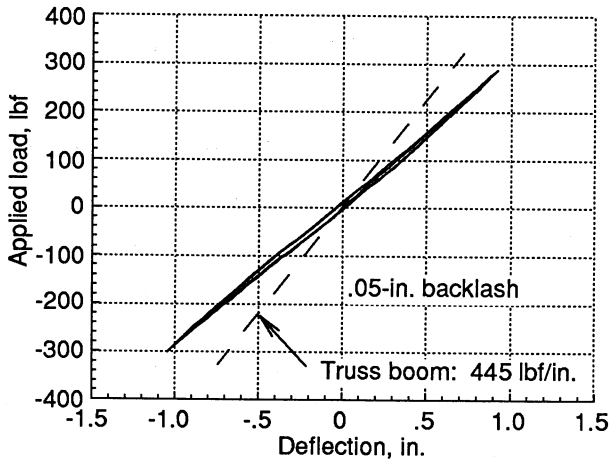

(b) Elbow joint with actuators replaced by steel tubes.

Figure 10. Load-deflection response of elbow joint test hardware.

the kinematic performance of the joint and are not flight-quality components.

Figure 10(a) shows the static load-deflection behavior for the first-generation elbow joint. The joint was tested at a 0° articulation angle to compare the results with those obtained for the truss boom. (See fig. 8.) The load cycle applied to the elbow joint was the same as that applied to the truss boom. The best-fit slope of the load-deflection curve when the load is positive is about 258 lbf/in., which is 41 percent less than that of the truss boom. (See fig. 8.) The joint load-deflection curve exhibits some nonlinearity, hysteresis, and backlash. The backlash, due to loose-fitting pins in the hinge and loose-fitting balls in the drive screw of the actuator, is estimated to be 0.09 in. This value was obtained by performing a best linear fit through the data when the load is positive and another through the data when the load is negative. The difference in the best-fit values at the abscissa was taken as the backlash.

To separate the amount of backlash in the joint hinges from the amount in the actuator drive screw, the actuators were replaced with 2-in-diameter steel tubes with wall thicknesses of 0.25 in., and a second static load-deflection test was performed. The axial stiffness of the steel tube was not matched to the original actuators. The load-deflection curve for this test (fig. 10(b)) shows a significant reduction in the nonlinearity, hysteresis, and backlash. As indicated on the figure, a backlash of 0.05 in. was measured with the technique previously described. This remaining backlash is attributed to looseness in the pins of the hinge joints. Currently, studies are being performed to evaluate the load-displacement behavior of actuators with close-fitting balls in the actuator drive screw.

The primary factor in designing the elbow joint shown in figure 9 was kinematic performance, which included actuator stroke ratio and actuator authority (defined as the change in actuator length required to provide 1° of joint articulation). Recently, a study was conducted (ref. 20) to develop a second-generation articulating joint for which both kinematic performance and improved stiffness were the primary design factors. The three articulating-truss joint concepts shown in figure 11 were evaluated in the study. Several features of these joints are similar to those in the joint test hardware shown in figure 9. Each of these joint concepts uses a single pair of variable-length actuators connected in series to achieve large-angle joint articulation, and the truss bays, which contain the actuators, have only three longerons. However, the three concepts shown in figure 11 use three different transition truss configurations to connect the four-longeron truss booms to the three-longeron articulating-truss joints. The major structural elements, such as the actuators, single-DOF hinge nodes, and truss struts, are common to the three joint concepts.

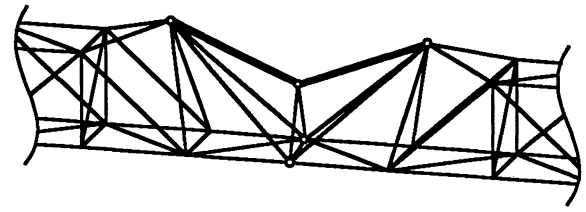

(a) Joint concept A.

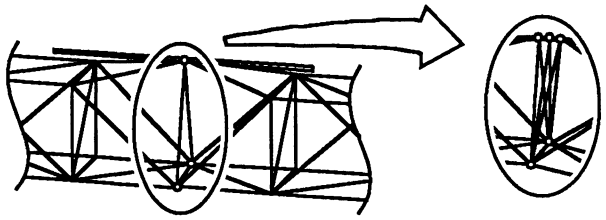

(b) Joint concept B.

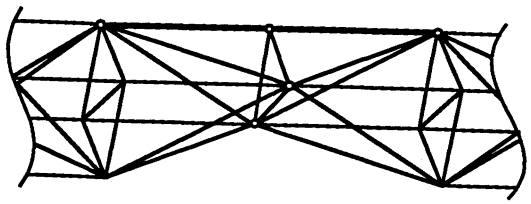

(c) Joint concept C.

Figure 11. Elbow joint concepts.

In the study, the kinematic and structural performance of each of the three joint concepts was evaluated as a function of geometric design parameters (ref. 20). One objective of the study was to select, for each joint concept, a specific geometric configuration that maintained the highest percentage of the reference truss stiffness across the joint, while still allowing large-angle articulation (at least 120°) with an actuator stroke ratio less than 2 (i.e., a single-fold actuator). The specific geometries selected are shown in figure 11. A second objective was to compare the structural dynamic performance of the three concepts and determine whether any significant differences exist. This objective was accomplished by determining the dynamic behavior of a 46-ft-long cantilever truss beam, with an articulating joint at the midspan, as a function of joint articulation angle for each of the three joint concepts. Figure 12 shows the fundamental natural frequencies of the

articulating truss beam for each concept with and without a tip mass. The fundamental frequency for all the concept models without a tip mass is about 2.2 Hz, and the frequency with a tip mass is about 0.6 Hz. All curves are relatively flat over the entire 120° articulation range. The mode shape for all three joint concepts (with and without a tip mass) at 0° articulation angle is first cantilever bending. As the joint is rotated to 120°, the fundamental mode shape changes to torsion in the root truss boom for concepts A and B and to bending about the joint-hinge axis for concept C. The three articulating-truss joint concepts analyzed in reference 20 had similar static and dynamic structural performance despite significant differences in their geometries. Therefore, this analysis leads to the conclusion that criteria other than structural or kinematic performance can be used as a basis for selecting among them.

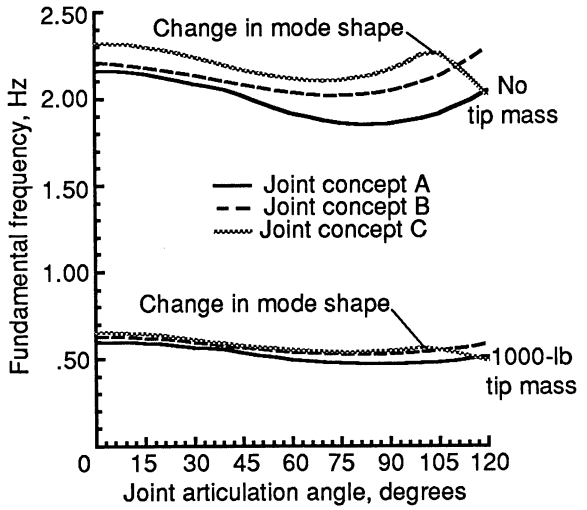

Figure 12. Fundamental natural frequencies for elbow joint concepts A, B, and C with and without a tip mass.

Rotary joint. A rotary joint is used to provide a rotational degree of freedom around the space crane boom axis. (See fig. 2.) The rotary joint concept shown in figure 13 was proposed during the preliminary design phase of Space Station *Freedom* to slew the solar arrays. Several point design studies (ref. 21) of the joint were conducted for cubic-truss bay sizes of about 16.4 ft. This rotary joint consists of transition truss members, an annular ring, eight bearing assemblies, and cross-tie members. The transition truss members connect the truss booms to the annular ring and bearing assemblies. Each side of the annular ring has 12 transition truss members for a total of 24 members. The cross-tie members provide additional stiffness where the transition truss members connect to the discrete-bearing assemblies. The transition truss and cross-tie members use the same type of erectable joint hardware as the truss booms to take advantage of structural predictability and ease of on-orbit assembly. A mechanism comprised of electrical motors and gearboxes would probably drive the rotary joint, and a brake would probably be used to hold the rotary joint at a desired orientation. Because the drive mechanism would not be in the structural load path of the rotary joint, the primary source of significant nonlinear structural behavior will probably be the discrete-bearing assemblies.

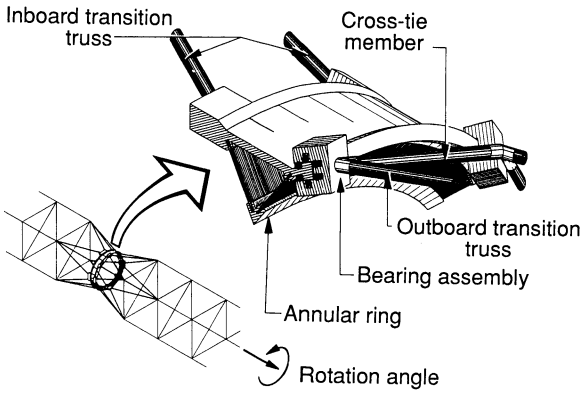

Figure 13. Discrete-bearing rotary joint concept.

The rotary joint structural performance is important because the joint should provide the strength and stiffness of an equivalent length of truss without a substantial increase in structural mass. The joint experiences the same loads as the truss it replaces, and as a result, each joint has to be designed to withstand those loads. The transition struts, for example, should be designed so that the Euler buckling load is greater than the loads experienced during space crane operations. Other design parameters that determine the structural performance of the rotary joint include the annular ring diameter and thickness, the transition truss member axial stiffness, and whether the rotary joint length is the equivalent of one or two bays of the truss boom. To assess the joint performance as a function of these design parameters, analytical studies were conducted to assess the dynamic characteristics of a truss boom with and without the rotary joint (ref. 22). The design parameters were varied and the frequencies compared with the truss boom frequencies. Joint designs were considered acceptable when the frequencies approximated those of the truss boom. One important conclusion from this study was that the one-bay rotary joint concept was more desirable than the two-bay rotary joint concept because of the higher Euler buckling allowables of the shorter transition truss members. Another important conclusion was that the

difference in structural mass between the one- and two-bay rotary joint concepts is small if the annular ring diameter is greater than 10 ft, as shown in figure 14. However, a considerable structural mass penalty is incurred by both the one- and the two-bay joint when the ring diameter becomes small.

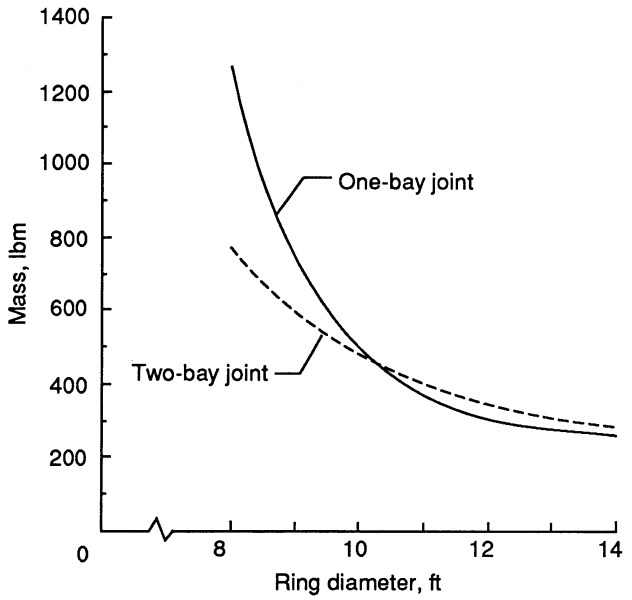

Figure 14. Mass of one- and two-bay rotary joints as a function of ring diameter.

Operational Considerations

Reach Envelope

In general, the reach envelope required for the space crane is a function of many parameters, such as the size of the spacecraft being assembled, whether the crane is attached to an ISCF or the spacecraft, and whether the crane is mounted to a mobile transporter. A study (ref. 23) was conducted to determine the reach envelope for a 360-ft-long space crane that has a 16.4-ft cubic-bay truss size and is attached to a representative construction facility. Two- and three-boom configurations were considered in the study, and the three-boom configuration is shown in figure 2. The reach envelope was obtained by rotating each of the elbow joints sequentially in increments of 10°, calculating the crane tip location at each increment, and superimposing the results onto the construction facility work area. Because the rotary joint was not rotated for this study, only a planar section of the reach envelope was defined.

Figure 15 shows the reach envelope sections produced by the three-boom space crane when the maximum elbow joint articulation angle is limited to 90°

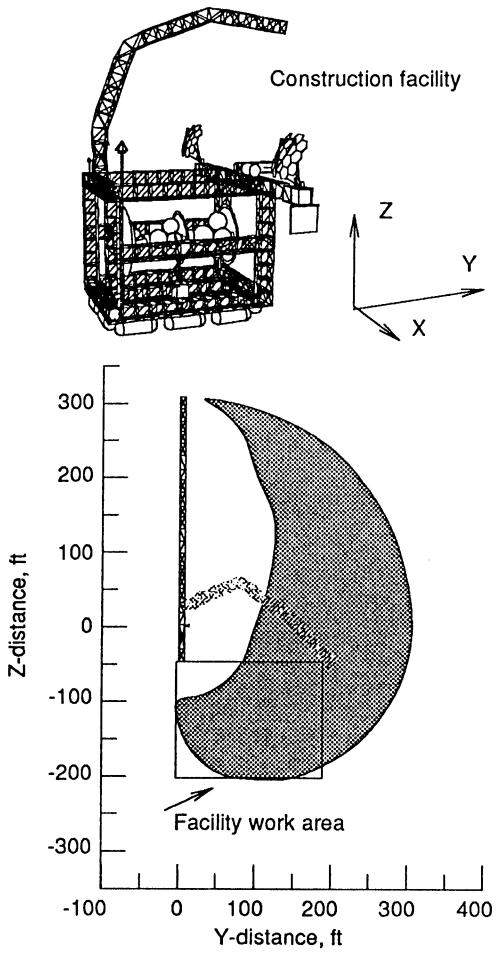

(a) Maximum joint angle = 90°.

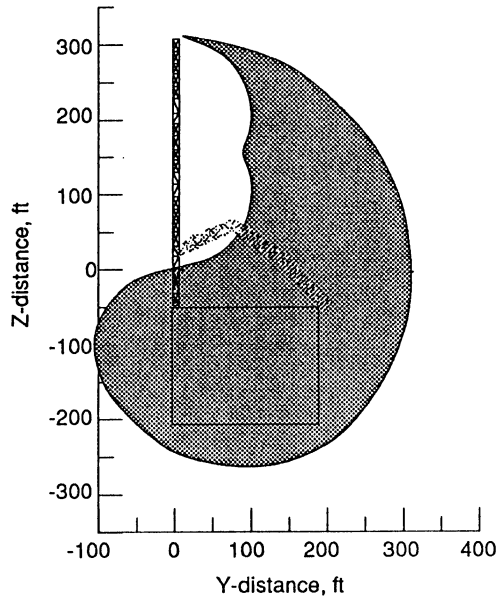

(b) Maximum joint angle = 120°.

Figure 15. Computed space crane reach envelope subject to elbow joint articulation constraints.

and to 120°. The figure also shows a side projection of the construction facility used to define the reach requirements. By increasing the maximum joint angle from 90° to 120°, the entire construction facility work area can be reached, as indicated by the envelope in figure 15(b). As the maximum joint angle increases, the total area within the reach envelope section also increases. Based on this study, the space crane must have at least three booms and elbow joints with maximum joint angles of at least 120° to reach all locations within the construction facility work area and to maintain an actuator stroke ratio of less than 2 in the elbow joints.

Rigid-Body Positioning

The simplest method for positioning the space crane tip is open-loop control of the actuators in the rotary and articulating joints. Because the erectable truss hardware is linear and predictable, the open-loop positioning precision of the space crane will probably be limited by the accumulated backlash present in the articulating joints. Reducing or eliminating the backlash in the articulating-truss joint components may allow adequate rigid-body tip-positioning accuracy to be achieved with a simple open-loop control system. The accuracy that can be obtained with this approach has not yet been determined experimentally.

The major loads in the space crane will probably be induced from accelerating and decelerating massive payloads during positioning operations. Accounting for the effects of these loads on the structure represents one method to define an open-loop control scheme for the space crane. An example of this method is to determine the maximum rate at which an articulating-truss joint can be rotated without buckling any members in the space crane. (See fig. 16(a).) In this analytical study, a sine function (fig. 16(b)) was chosen as the joint rotation profile for the elbow joint shown in figure 9, and the time required to reach a 1-rad angle was varied from 5 to 60 sec. Three different tip masses (0, 2204, and 11 023 lbm) were studied, and the peak bending moment at the root was computed and converted into an equivalent axial force in the four root-bay longerons. As shown in figure 16(c), considering Euler buckling of the truss members limits the minimum slew time for a 2204-lbm tip mass to about 8 sec. For slew times on the order of 60 sec, the peak member forces are about 10 percent of the longeron Euler buckling load (1216 lbf) for all the tip masses studied. Similar analyses can be used to define open-loop slew rates for other joint rotation profiles. Other failure criteria, such as the maximum dynamic force in a passive damping structural member, can also be used to define open-loop control profiles with this method.

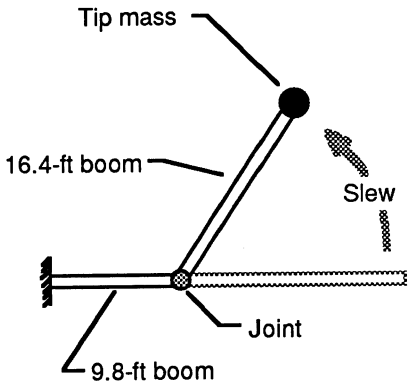

(a) Dynamic analysis model.

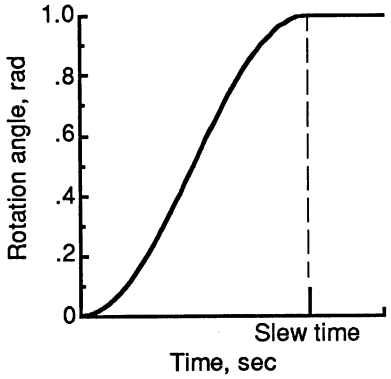

(b) Slew maneuver profile.

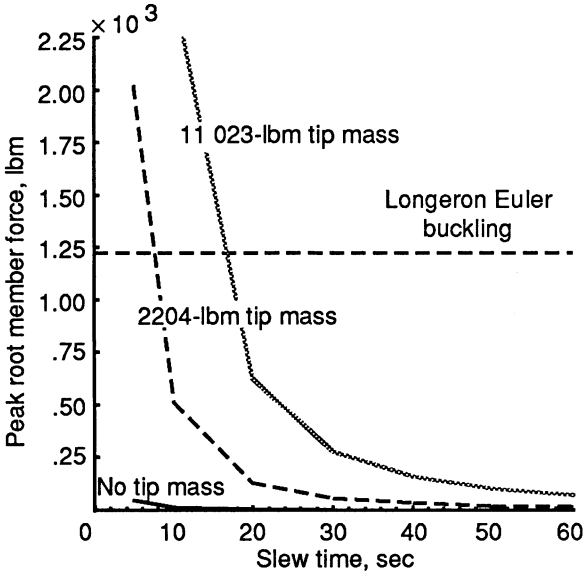

(c) Peak force in root-bay longeron as a function of slew time.

Figure 16. Peak force in root truss member as a function of slew time for elbow articulating-truss joint.

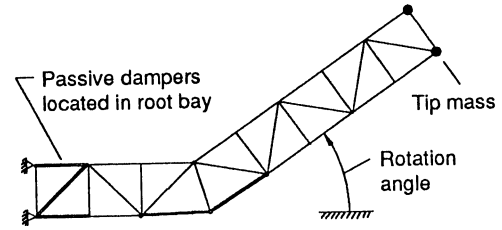

(a) Dynamic analysis model.

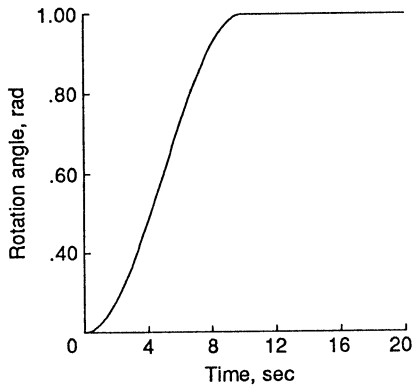

(b) Slew maneuver time history.

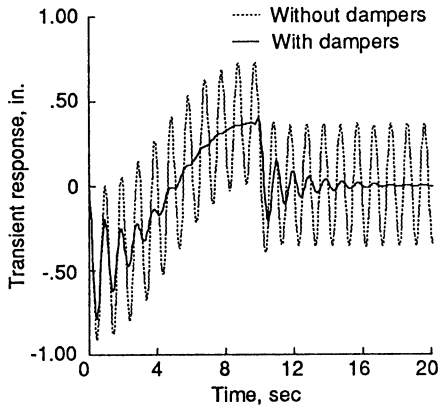

(c) Tip transient response.

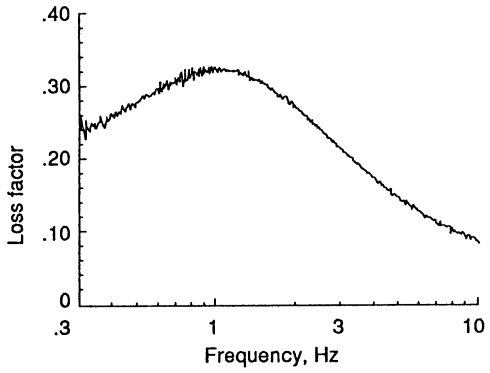

(d) Passive damper effectiveness.

Figure 17. Vibration response of elbow joint model with and without damping augmentation.

Vibration Suppression

As noted previously, the erectable truss hardware has little inherent damping. Therefore, damping augmentation may be necessary for vibration suppression in the space crane. The following hierarchical strategy for improving vibration suppression (in increasing order of complexity) can be implemented: passive damping, preshaped command input (PSCI), and active vibration suppression. One approach to vibration suppression is to replace selected truss members with structural elements that contain passive dampers. For example, devices that are capable of resisting static loads in addition to providing substantial amounts of viscous damping have been designed and space-qualified components have been fabricated (refs. 24 and 25). Figure 17 shows an example of the damping augmentation that might be achieved with these dampers. An analytical model of the elbow joint (fig. 9) with a 2204-lbm tip mass (fig. 17(a)) is slewed through 1 rad in 10 sec (fig. 17(b)). The undamped tip displacement is shown as a dashed line in figure 17(c). When passive dampers (with a representative damping coefficient of 8000 lbf-sec/in.) are included in the three truss members of the root truss bay (fig. 17(a)), the tip deflection is greatly reduced (the solid line in fig. 17(c)). The viscous dampers described in references 24 and 25 also exhibit significant damping over a wide frequency range, as shown by the test data in figure 17(d). This feature is important because the natural frequencies of the space crane change as the payload and the position are varied.

Another technique for vibration suppression is preshaped command input. The PSCI is an open-loop technique based on the principle that the system input (e.g., actuator commands) can be modified so as not to excite responses of selected structural frequencies (ref. 26). By modifying the actuator extension rate, the space crane is able to complete a specified move and have little residual motion at the end of the move. This technique has several advantages: it is simple to implement because it requires knowledge of only the system frequencies (not the mode shapes) and it is an open-loop approach. Another advantage is that the performance can be designed such that it is insensitive to frequency or damping ratio over a specified bandwidth. Also, multiple modes can be suppressed simultaneously (ref. 27). Figure 12 shows that for certain space crane configurations, the crane fundamental frequency remains fairly constant as booms are rotated for an unloaded crane and for a crane with a tip mass, even though the mode shape is changing. (See refs. 20 and 23.) Thus, an input modified to suppress residual motion induced by the

fundamental frequency would be effective throughout that entire range of motion of the space crane.

Passive damping systems are easier to implement and less costly to develop than active systems. Thus, current space crane research focuses on the techniques of augmented passive damping and PSCI. Analyses performed to date indicate that these techniques greatly enhance the structural damping in the space crane and may be adequate for vibration suppression. Thus, active vibration control methods need only be considered if the simpler methods described previously are not adequate.

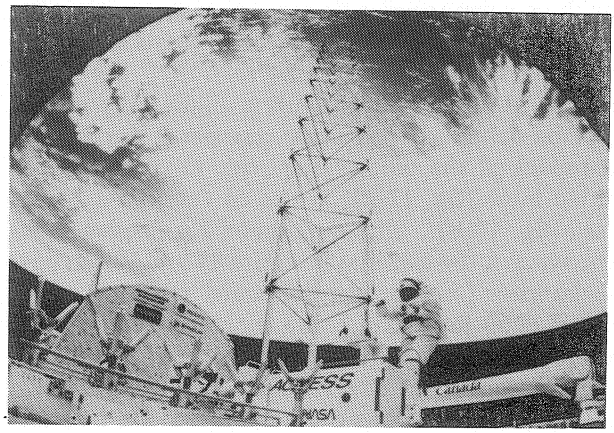

(a) ACCESS experiment.

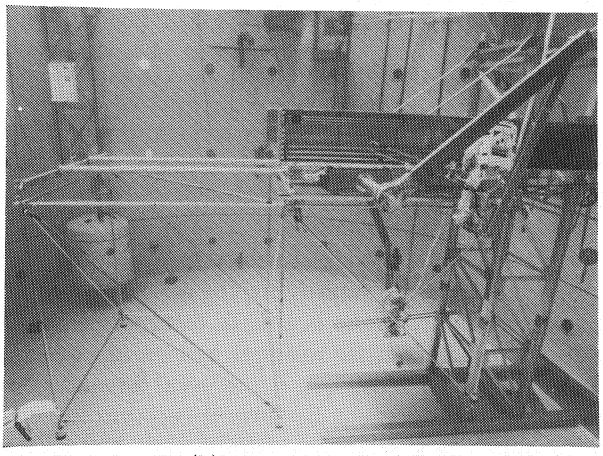

(b) Mobile transporter.

Figure 18. Erectable truss assembly experiments.

Crane Construction on Orbit

The truss members and nodes for the space crane package compactly for transportation to orbit, and proven techniques exist for assembling them on orbit. For example, the Assembly Concept for Construction of Erectable Space Structures (ACCESS) experiment was performed in the cargo bay of the Space Shuttle *Atlantis* in November 1985 (ref. 28). In the baseline experiment, two astronauts working from fixed foot restraints were able to assemble a 45-ft-long, 189-lbm truss beam consisting of 93 struts as shown in figure 18(a). The battens and longerons in the truss were 4.5 ft long, the diagonals were 6.36 ft long, and the struts were 1 in. in diameter. The assembly rate for this truss was about 17 sec/strut.

A larger scale truss has also been assembled with the aid of a mobile transporter in neutral buoyancy tests (ref. 17), as shown in figure 18(b). In these tests, a three-bay cubic truss configuration (consisting of forty-four 2-in-diameter struts that were 15 ft long) was assembled by a pair of test subjects in a simulated space environment. Working from a mobile transporter, the assembly rate for this large truss was about 28 sec/strut.

Small space cranes (bay sizes of ≈30–80 in.) could be efficiently assembled by astronauts on orbit with a minimum of infrastructure, as with ACCESS. Larger space cranes could be efficiently assembled by astronauts augmented with aids such as a mobile transporter. For example, the large space crane truss structure shown in figure 2 could be assembled in a little over 2 hours with the mobile transporter (ref. 17). In the future, telerobotic techniques using the tip manipulator system described in reference 29 could also be used to assemble the space crane on orbit.

Concluding Remarks

Many future human space exploration missions will probably require large vehicles that must be assembled on orbit. The exact specifications of these large spacecraft and the types of on-orbit operations required are not well-defined. However, a device that can move, position, and assemble large and massive spacecraft components on orbit becomes essential to support these missions. Current and proposed space manipulators do not have the capabilities that are anticipated to be required; therefore, space crane concepts for large-scale on-orbit assembly are being developed. These concepts incorporate the following key features: they are reconfigurable to meet changing needs, their structural behavior is predictable to reduce ground test requirements and to simplify the rigid-body control system design, they have large load capability and long reach, and passive damping is easily implemented. This paper describes a space crane concept that exhibits all these features. This concept incorporates three major elements: (1) a mobile base that can move around the work site, (2) a crane body that consists of booms and articulating joints to provide coarse tip positioning over large distances, and (3) a tip manipulator

system that provides additional dexterity and precisely positions payloads.

Using erectable truss hardware makes the space crane structural concept generic because the hardware can be reconfigured into different geometries and sizes. Static and dynamic tests have established that the hardware has linear and predictable structural performance. Thus, the space crane structural behavior can be accurately predicted with linear analysis. Articulating-truss joint concepts with significantly different geometries were analyzed and found to have similar static and dynamic performance; thus, criteria other than structural and kinematic performance can be used to select a joint. One- and two-bay rotary joints were also shown to have little difference in structural efficiency. However, the one-bay rotary joint is more desirable because its shorter transition truss members have higher Euler buckling loads. Finally, passive damping and the open-loop preshaped command input technique greatly enhance the structural damping in the space crane and may preclude the need for an active vibration suppression system.

NASA Langley Research Center
Hampton, VA 23681-0001
November 3, 1992

References

1. Report of the National Commission on Space: *Pioneering the Space Frontier.* Bantam Books, Inc., 1986.

2. *The Office of Exploration FY 1989 Annual Report—Exploration Studies Technical Report. Volume II: Space Transportation Systems.* NASA TM-4170, 1989.

3. Synthesis Group on America's Space Exploration Initiative: *America at the Threshold.* U.S. Government Printing Off., c.1991.

4. Mikulas, Martin M., Jr.; and Dorsey, John T.: *An Integrated In-Space Construction Facility for the 21st Century.* NASA TM-101515, 1988.

5. Bush, Harold G.; Lake, Mark S.; Watson, Judith J.; and Heard, Walter L., Jr.: *The Versatility of a Truss Mounted Mobile Transporter for In-Space Construction.* NASA TM-101514, 1988.

6. Gossain, D. M.; and Smith, P. J.: Structural Design and Test of the Shuttle RMS. *Environmental Effects on Materials for Space Applications,* AGARD-CP-327, Mar. 1983, pp. 2-1–2-10.

7. Graham, J. D.; Ravindran, R.; and Knapp, K.: Space Manipulators—Present Capability and Future Potential. *A Collection of Technical Papers—AIAA/NASA Conference on Advanced Technology for Future Space Systems,* American Inst. of Aeronautics and Astronautics, Inc., May 1979, pp. 243–253. (Available as AIAA Paper 79-0903.)

8. Hunter, J. A.; Ussher, T. H.; and Gossain, D. M.: Structural Dynamic Design Considerations of the Shuttle Remote Manipulator System. *A Collection of Technical Papers, Part 1—23rd Structures, Structural Dynamics and Materials Conference,* May 1982, pp. 499–505. (Available as AIAA-82-0762.)

9. Grumman Space Station Div.: *Robotic Systems Functional/Performance Assessment.* SSC 18400 (Contract NASW-4300), Sept. 15, 1991.

10. McCain, Harry G.; Andary, James F.; Hewitt, Dennis R.; and Haley, Dennis C.: The Space Station *Freedom* Flight Telerobotic Servicer: The Design and Evolution of a Dexterous Space Robot. IAF-90-076, Oct. 1990.

11. Andary, James F.; Hewitt, Dennis R.; Spidaliere, Peter D.; and Lambeck, Robert W.: Characteristics and Requirements of Robotic Manipulators for Space Operations. *Proceedings on Cooperative Intelligent Robotics in Space II,* Volume 1612, William E. Stoney, ed., Soc. of Photo-Optical Instrumentation Engineers, 1991, pp. 13–23.

12. Hughes, Peter C.; Sincarsin, Wayne G.; and Carroll, Kieran A.: "Trussarm"—A Variable-Geometry-Truss Manipulator. *First Joint U.S./Japan Conference on Adaptive Structures,* Ben K. Wada, James L. Fanson, and Koryo Miura, eds., Technomic Publ., Co., Inc., c.1991, pp. 715–725.

13. Rhodes, Marvin D.; and Mikulus, Martin M., Jr.: *Deployable Controllable Geometry Truss Beam.* NASA TM-86366, 1985.

14. Mikulas, M. M., Jr.; Davis, R. C.; and Greene, W. H.: *A Space Crane Concept: Preliminary Design and Static Analysis.* NASA TM-101498, 1988.

15. Bush, Harold G.; Herstrom, Catherine L.; Heard, Walter L., Jr.; Collins, Timothy J.; Fichter, W. B.; Wallsom, Richard E.; and Phelps, James E.: Design and Fabrication of an Erectable Truss for Precision Segmented Reflector Application. AIAA-90-0999, Apr. 1990.

16. Sutter, Thomas R.; Wu, K. Chauncey; Riutort, Kevin T.; Laufer, Joseph B.; and Phelps, James E.: *Structural Characterization of a First-Generation Articulated-Truss Joint for Space Crane Application.* NASA TM-4371, 1992.

17. Watson, Judith J.; Bush, Harold G.; Heard, Walter L., Jr.; Lake, Mark S.; Jensen, J. Kermit; Wallsom, Richard E.; and Phelps, James E.: Mobile Transporter Concept for Extravehicular Activity Assembly of Future Spacecraft. *J. Spacecr. & Rockets,* vol. 29, no. 4, July–Aug. 1992, pp. 437–443.

18. Ring, L. R.: *Process Development and Fabrication of Space Station Type Aluminum-Clad Graphite Epoxy Struts.* NASA CR-181873, 1990.

19. Bowles, David E.; and Tenney, Darrel R.: Composite Tubes for the Space Station Truss Structure. *Materials for Space—The Gathering Momentum, 18th International*

SAMPE Technical Conference, Soc. for the Advancement of Material and Process Engineering, 1986, pp. 414–428.

20. Wu, K. Chauncey; and Sutter, Thomas R.: *Structural Analysis of Three Space Crane Articulated-Truss Joint Concepts.* NASA TM-4373, 1992.

21. Systems Engineering and Integration Space Station Program Office: *Space Station Reference Configuration Description.* JSC-19989, NASA Lyndon B. Johnson Space Center, Aug. 1984. (Available as NASA TM-87493.)

22. Vail, J. Douglas; and Lake, Mark S.: *Comparison of Structural Performance of One- and Two-Bay Rotary Joints for Truss Applications.* NASA TM-4282, 1991.

23. Sutter, Thomas R.; Bush, Harold G.; and Wallsom, Richard E.: An Articulated-Truss Space Crane Concept. *A Collection of Technical Papers, Part 4—AIAA/ASME/ASCE/AHS/ASC 31st Structures, Structural Dynamics and Materials Conference,* Apr. 1990, pp. 2117–2125. (Available as AIAA-90-0994-CP.)

24. Davis, L. Porter; and Ginter, Steven D.: An Advanced D-Strut™. *Proceedings of Damping '91,* WL-TR-91-3078, Vol. III, U.S. Air Force, Aug. 1991, pp. IAC-1–IAC-17. (Available from DTIC as AD A241 313.)

25. Davis, L. Porter; Workman, Brian J.; Chu, Cheng-Chih; and Anderson, Eric H.: Design of a D-Strut™ and Its Application Results in the JPL, MIT, and LaRC Test Beds. Honeywell paper presented at the American Institute of Aeronautics and Astronautics Structural Dynamics Meeting (Dallas, Texas), Apr. 13, 1992.

26. Singer, N. C.; and Seering, W. P.: Preshaping Command Inputs To Reduce System Vibration. *Trans. ASME: J. Dyn. Syst., Meas., & Control,* vol. 112, Mar. 1990, pp. 76–82.

27. Hyde, James M.; and Seering, Warren P.: Using Input Command Pre-Shaping To Suppress Multiple Mode Vibration. *Proceedings 1991 IEEE International Conference on Robotics and Automation,* Volume 3, IEEE Catalog No. 91CH2969-4, IEEE Computer Soc., 1991, pp. 2604–2609.

28. Heard, Walter L., Jr.; Watson, Judith J.; Ross, Jerry L.; Spring, Sherwood C.; and Cleave, Mary L.: Results of the ACCESS Space Construction Shuttle Flight Experiment. *A Collection of Technical Papers—AIAA Space Systems Technology Conference,* American Inst. of Aeronautics and Astronautics, June 1986, pp. 118–125. (Available as AIAA-86-1186.)

29. Rhodes, Marvin D.; and Will, Ralph W.: Automated Assembly of Large Scale Structures. IAF Paper No. 90-272, Oct. 1990.

REPORT DOCUMENTATION PAGE

Form Approved
OMB No. 0704-0188

1. AGENCY USE ONLY *(Leave blank)*	2. REPORT DATE	3. REPORT TYPE AND DATES COVERED
	November 1992	Technical Paper

4. TITLE AND SUBTITLE
Structurally Adaptive Space Crane Concept for Assembling Space Systems on Orbit

5. FUNDING NUMBERS
WU 506-43-41-02

6. AUTHOR(S)
John T. Dorsey, Thomas R. Sutter, and K. Chauncey Wu

7. PERFORMING ORGANIZATION NAME(S) AND ADDRESS(ES)
NASA Langley Research Center
Hampton, VA 23681-0001

8. PERFORMING ORGANIZATION REPORT NUMBER
L-17175

9. SPONSORING/MONITORING AGENCY NAME(S) AND ADDRESS(ES)
National Aeronautics and Space Administration
Washington, DC 20546-0001

10. SPONSORING/MONITORING AGENCY REPORT NUMBER
NASA TP-3307

11. SUPPLEMENTARY NOTES

12a. DISTRIBUTION/AVAILABILITY STATEMENT
Unclassified–Unlimited

Subject Category 18

12b. DISTRIBUTION CODE

13. ABSTRACT *(Maximum 200 words)*

Many future human space exploration missions will probably require large vehicles that must be assembled on orbit. Thus, a device that can move, position, and assemble large and massive spacecraft components on orbit becomes essential for these missions. This paper describes a concept for such a device—a space crane concept that uses erectable truss hardware to achieve high-stiffness and low-mass booms and uses articulating-truss joints that can be assembled on orbit. The hardware has been tested and shown to have linear load-deflection response and to be structurally predictable. The hardware also permits the crane to be reconfigured into different geometries to satisfy future assembly requirements. A number of articulating and rotary joint concepts have been sized and analyzed, and the results are discussed in this paper. Two strategies have been proposed to suppress motion-induced vibration: placing viscous dampers in selected truss struts and preshaping motion commands. Preliminary analyses indicate that these techniques have the potential to greatly enhance structural damping.

14. SUBJECT TERMS	15. NUMBER OF PAGES
Space structures; Space crane; On-orbit assembly; Truss structures; Adaptive structures	19
	16. PRICE CODE A03

17. SECURITY CLASSIFICATION OF REPORT	18. SECURITY CLASSIFICATION OF THIS PAGE	19. SECURITY CLASSIFICATION OF ABSTRACT	20. LIMITATION OF ABSTRACT
Unclassified	Unclassified		

NSN 7540-01-280-5500

Standard Form 298(Rev. 2-89)
Prescribed by ANSI Std. Z39-18
298-102

NASA-Langley, 1992